

# Assembly of high-potency photosensitiser-antibody conjugates through application of dendron multiplier technology.

Francesca Bryden,<sup>[a]</sup> Antoine Maruani,<sup>[b]</sup> João M.M. Rodrigues,<sup>[c]</sup> Miffy H.Y. Cheng,<sup>[c]</sup> Huguette Savoie,<sup>[c]</sup> Andrew Beeby\*,<sup>[d]</sup> Vijay Chudasama\*,<sup>[b]</sup> Ross W. Boyle\*<sup>[c]</sup>

---

[a] Dr F. Bryden, UMR7292 GICC CNRS-Univer(té de Tours, Team IMT, 31 Avenue Monge, 37200 Tours, France.

[b] Dr V. Chudasama, Dr A. Maruani, Department of Chemistry, University College London, 20 Gordon Street, London, WC1H 0AJ, UK.  
Email: v.chudasama@ucl.ac.uk

[c] Dr J.M.M. Rodrigues, M.H.Y. Cheng, H. Savoie, Prof. R.W. Boyle, Department of Chemistry, University of Hull, Cottingham Road, Hull, HU6 7RX, UK.

E-mail: r.w.boyle@hull.ac.uk

[d] Dr A. Beeby, Department of Chemistry, University of Durham, Durham DH1 3LE, UK.  
Email: andrew.beeby@durham.ac.uk

## Abstract

Exploitation of photosensitisers as payloads for antibody-based anti-cancer therapeutics offers a novel alternative to the small pool of commonly-utilised cytotoxins. However, existing bioconjugation methodologies are incompatible with the requirement of increased antibody loading without compromising antibody function, stability or homogeneity. Herein, we describe the first application of dendritic multiplier groups to allow the loading of more than 4 porphyrins to a full IgG antibody in a site-specific and highly homogeneous manner. Photophysical evaluation of UV-visible absorbance and singlet oxygen quantum yields highlighted porphyrin-dendron **14** as the best candidate for bioconjugation; with subsequent bioconjugation producing a HER2-targeted therapeutic with average loading ratios of 15.4:1. *In vitro* evaluation of conjugate **18** demonstrated a nanomolar photocytotoxic effect in a target cell line, which overexpresses HER2, with no observed photocytotoxicity at the same concentration in a control cell line which expresses native HER2 levels, or in the absence of irradiation with visible light.

## Introduction

The field of antibody-drug conjugates (ADCs) has experienced an explosion of research interest in recent years, with three clinically-approved drugs (Adcetris<sup>®</sup>, Kadyla<sup>®</sup> and Besponsa<sup>®</sup>) and over 60 other ADCs currently undergoing clinical trials<sup>1</sup>. Despite this, the variety of payloads utilised is limited, with over two thirds of ADCs exploiting just two classes of cytotoxic agents; auristatins and maytansinoids<sup>2</sup>. One potential avenue to increase payload diversity lies in the field of photoimmunotherapeutic agents; tumour-associating antibodies loaded with photosensitisers. The exploitation of photosensitisers in photodynamic therapy (PDT) offers a completely novel mechanism of action; these drugs exhibit cytotoxic action only under irradiation with visible light, producing reactive oxygen species, most notably singlet oxygen, and resulting in a secondary cytotoxic action

Although many examples of photoimmunotherapeutic agents exist<sup>3</sup>, their utility is limited by the bioconjugation methodologies used. For targeted PDT, conjugation to antibodies is typically achieved through lysine modification, however lysine modification is suboptimal as it generates heterogeneous products, which can result in batch-to-batch variability and poor pharmacokinetics. Cysteine modification, following inter-chain disulfide reduction is another viable strategy, however this results in the permanent loss of structural disulfide bonds, which may reduce the stability of the antibody

conjugate *in vivo*. Moreover, cysteine modification is often carried out by reaction with classical maleimide compounds. Whilst this reaction is reliable, it has been widely reported (and proven in various guises) that the formed succinimide conjugate is unstable in serum, due to the propensity of this motif to undergo retro-conjugate addition<sup>4-8</sup>. This subsequently leads to undesirable transfer of the attached cargo onto blood thiols, particularly human serum albumin, thus resulting in off-target delivery. Herein we report the use of pyridazinediones<sup>9, 10</sup> to functionalise the native solvent accessible interstrand disulfide bonds in trastuzumab to yield validated serum stable antibody conjugates with exactly 4 pyridazinediones per full antibody.

We have previously shown that the application of re-bridging technologies in order to conjugate to interchain disulfide bridges is a powerful tool for circumventing many of the challenges associated with porphyrin ADCs,<sup>11, 12</sup> allowing for targeted photocytotoxicity, while maintaining precise loading ratios and binding affinity. However, this technology was primarily designed for the generation of highly cytotoxic ADCs, for which the EC<sub>50</sub> of the toxic payload is in the nanomolar range, or lower. In such ADCs, the generated drug-to-antibody ratio (DAR) of *ca.* 4 allows for excellent potency, with higher loading causing aggregation and rapid clearance *in vivo* due to the lipophilic nature of the drug.

In contrast, the EC<sub>50</sub> of porphyrins for PDT is significantly higher (typically in the micromolar range).<sup>13</sup> As a result, porphyrin ADCs would benefit from the development of technologies which permit higher loading ratios, but which also overcome the inherent problems of direct lysine or cysteine conjugation (see above).

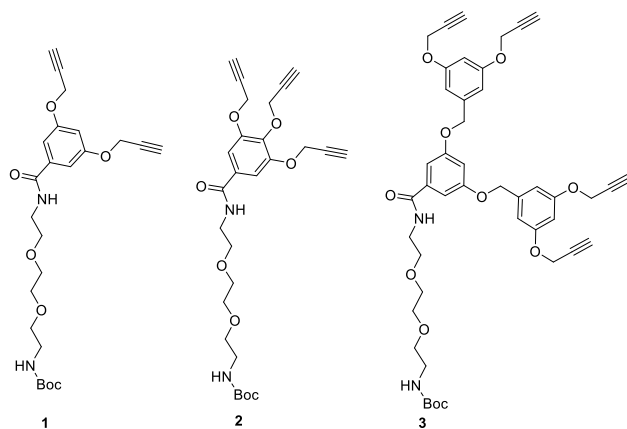
Multiple loading strategies incorporating branched dendron units have previously been exploited within ADCs, usually in combination with enzymatic coupling strategies to obtain a DAR of 4-8.<sup>14</sup> While use of multi-photosensitizer structures for PDT has also been demonstrated,<sup>15, 16</sup> in contrast, the application of dendron technology for targeted PDT has been attempted only once previously.<sup>17</sup> While the synthesized structures retained desirable photophysical characteristics, the harsh coupling conditions were applied only to highly hydrophobic porphyrins, and bioconjugation was not attempted.

To this end, we have developed a range of dendron structures bearing 2-4 alkyne functionalities. These can undergo the copper-catalysed azide-alkyne cycloaddition (CuAAC) reaction with azide-functionalised porphyrins, allowing mild attachment of water-soluble porphyrins in near-quantitative yields.<sup>18</sup> The photophysical potential of these structures as therapeutic payloads was evaluated, and bioconjugation and biological evaluation of the lead structure was demonstrated. This represents the first example of a homogenous re-bridging bioconjugation technology, which permits increased payload DAR of up to 16 on a native antibody.

## Results and Discussion

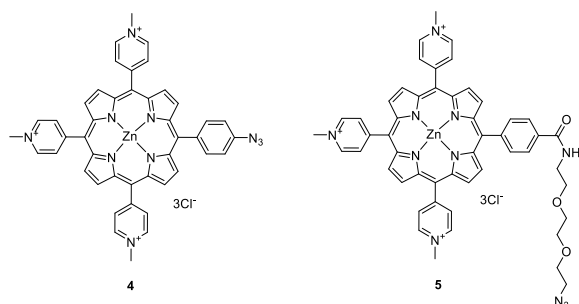
Initially, synthesis of a range of aryl ether dendrons **1-3** was carried out (Fig. 1), bearing 2-4 alkyne functional groups and a spacer chain bearing a protected amine group. For photophysical evaluation a short triethylene glycol spacer was used, engendering moderate hydrophilicity without the prohibitive cost of longer PEG chains. Synthesis of all intermediates was carried out using a literature method<sup>19</sup>, with the final addition of the triethylene glycol spacer carried out via peptide coupling to obtain the products in good yields.

**Figure 1.** Structures of aryl ether dendrons **1-3**. While **1** and **2** are single generation dendrons with 2 and 3 alkyne functionalities respectively, **3** is a second generation dendron with 4 alkyne functionalities.



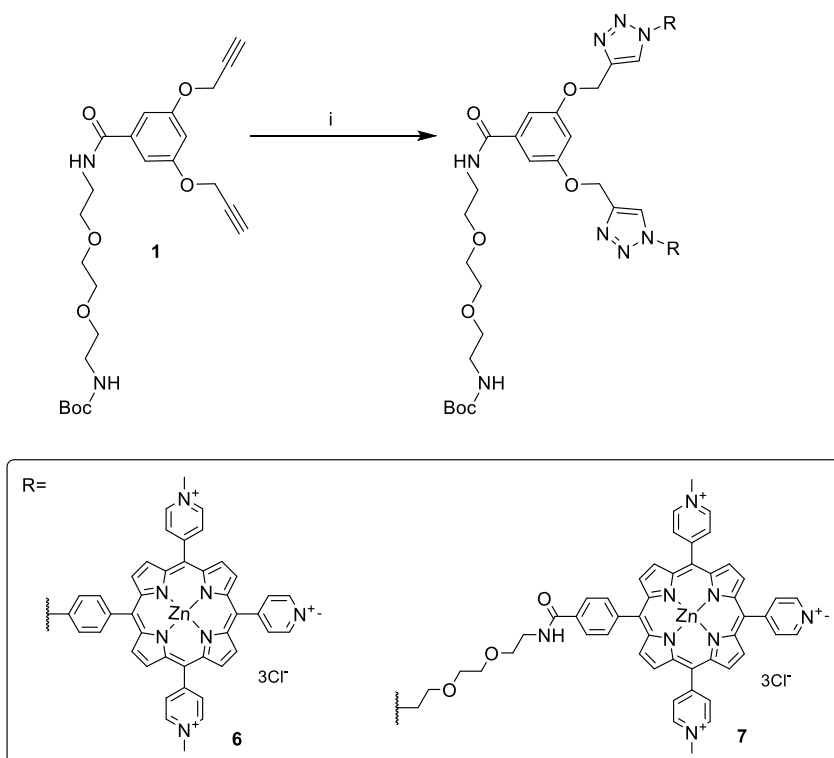
Porphyrins **4** and **5** have previously demonstrated excellent photocytotoxicity when attached to antibodies (Fig 2).<sup>12</sup> Thus, their potential for porphyrin–dendron generation was explored and conjugation of both **4** and **5** on dendrons **1-3** was attempted via CuAAC reaction, with mild microwave heating employed in each case.

**Figure 2.** Structures of hydrophilic porphyrins **4** and **5**



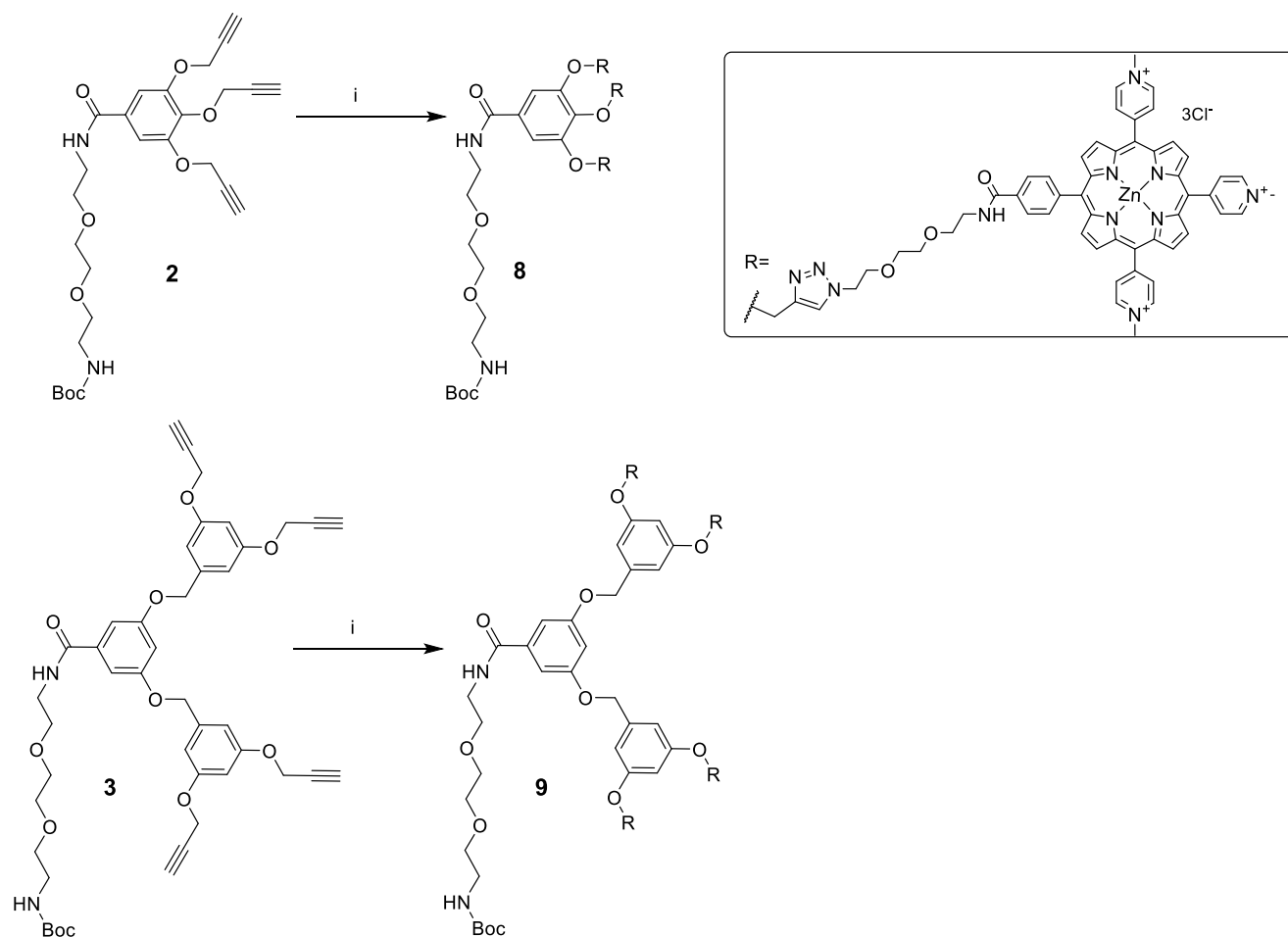
Reaction with dendron **1** proceeded well, with both porphyrins **4** and **5** rapidly reaching completion and requiring only simple workup without chromatographic purification, to produce products **6** and **7** (Fig. 3) in excellent yield and purity. In contrast, the conjugation between porphyrin **4** and both dendrons **2** and **3** proceeded poorly. After 1 hour, HPLC analysis of the crude mixture showed consumption of the starting dendron, and formation of a single product, however NMR analysis revealed the formation of a product with one fewer porphyrin attached than expected (**2** and **3** respectively). Reaction intensification, including extended reaction times, addition of an excess of porphyrin, and heating to 60°C showed no appreciable formation of the desired product in either case.

**Figure 3.** Synthetic scheme for dendrons **6** and **7**. i, porphyrin (**4** or **5**), CuSO<sub>4</sub>, NaAsc, Tris(1-benzyl-1H-1,2,3-triazol-4-yl)methyl]amine (TBTA), 40°C, MW.



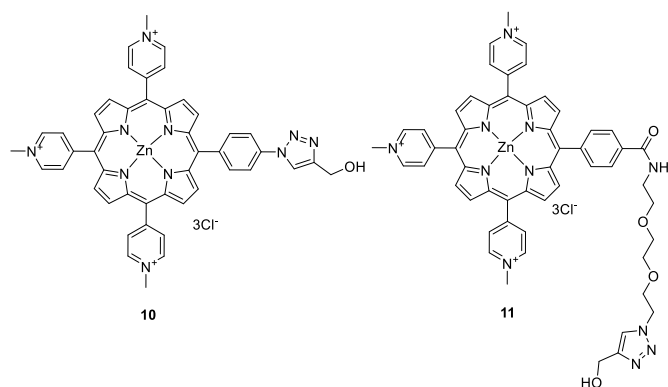
In contrast, reactions between porphyrin **5** and dendrons **2** and **3** proceeded rapidly to completion, with NMR analysis confirming the attachment of 3 and 4 porphyrins respectively (see ESI). The successful synthesis of **8** and **9** (Fig. 4) can therefore be attributed to reduced steric hindrance as a result of the flexible triethylene glycol spacer chain on porphyrin **5**, allowing more facile attachment of more than two porphyrin in the sterically hindered structure.

**Figure 4.** Synthetic scheme for dendrons **8** and **9**. i, **5**, CuSO<sub>4</sub>, NaAsc, TBTA, 40°C, MW.



Following synthesis of structures **6-9**, analysis of their photophysical properties was carried out. The close physical proximity of the porphyrins to one another and also to the central dendritic skeleton has the potential to lead to quenching of both the triplet excited state and generation of therapeutic singlet oxygen. As a result, both UV absorption of the principal Soret band, and singlet oxygen quantum yield ( $\Phi_{\Delta}$ ) for all porphyrins were evaluated, in comparison to control porphyrins **10** and **11** (Fig. 5) which were pre-reacted with propargyl amine to remove the reactive azide group. The UV-absorption of the Soret band was then divided by that of the relevant control porphyrin to obtain a UV absorption ratio for each porphyrin-dendron structure. In a perfect system, each porphyrin would retain identical photophysical characteristics in comparison to the control porphyrin, and thus the UV absorption ratio would be equivalent to that of the stoichiometry.

**Figure 5.** Structures of control porphyrins **10** and **11**.



The most significant difference in UV-visible absorption was observed for **6** (Table 1), with the reduction observed (*ca.* 30%) being unsurprising since this was the only structure to employ the more sterically-hindered porphyrin **4**. A modest reduction (*ca.* 10%) was also observed for **8**, which can be attributed the larger number of porphyrins in comparison to **7**. In comparison to **9**, while the number of porphyrins is smaller, the three porphyrins are arranged on the single generation dendron **2** rather than the second generation dendron **3**. A lack of this second layer of branching increases the proximity of the three porphyrins of **8**, and thus quenching is higher. In contrast to the other structures, **9** actually showed a small increase in UV absorption in comparison to the same stoichiometric quantity of the parent porphyrin. The reason for this effect is not known, however it is possible that the rigid structure of this second generation dendron allows for regular spacing between porphyrins to be maintained more easily than between free porphyrins in solution (which may have a tendency towards aggregation), allowing improved absorption characteristics.

**Table 1.** Photophysical data for structures **6-11**.

Structure	Stoichiometry <sup>[a]</sup>	$\Phi_{\Delta}$ <sup>[b]</sup>	UV absorption ratio <sup>[c]</sup>	$\Phi_{\Delta}$ , generation potential <sup>[d]</sup>
10	1	0.47	1	0.47
11	1	0.86	1	0.86
6	2	0.21	1.41	0.29
7	2	0.27	1.98	0.53
8	3	0.28	2.68	0.75
9	4	0.28	4.30	1.20

[a] As determined by NMR [b] Normalised  $\Phi_{\Delta}$  (in D<sub>2</sub>O) [c] Ratio of total UV absorption (in H<sub>2</sub>O) of structure to the absorption of the single porphyrin analogue. In a perfect system this would be equal to the stoichiometry. [d] Calculation of the singlet oxygen generation potential of the entire porphyrin-dendron system, calculated as a function of normalised  $\Phi_{\Delta}$  and UV absorption ratio.

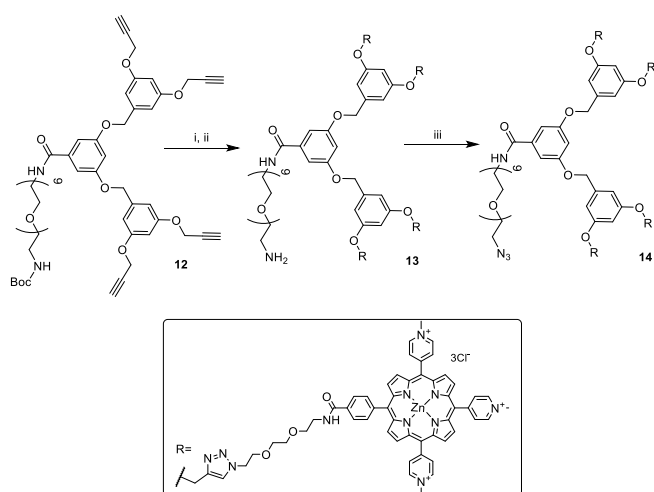
In general, it can be seen that the  $\Phi_{\Delta}$  values are highest for the control porphyrins **10** and **11**. The reduced  $\Phi_{\Delta}$  of **10** in comparison to **11** suggests that the proximity of the triazole ring also reduces the quantum yield, possibly as a result of direct quenching of the porphyrin. While all synthesised porphyrin-dendron conjugates demonstrated reduced  $\Phi_{\Delta}$  in comparison to the control porphyrins, a surprising lack of variation between the conjugates was observed. A minor change was again observed with the use of the PEG spacer, with an increase in  $\Phi_{\Delta}$  between **6** and **7**. However, no

significant difference in the  $\Phi_{\Delta}$  between **7**, **8** and **9** was observed, suggesting that the quenching in these systems is not significantly increased by the addition of subsequent porphyrins.

While it is evident that the porphyrin-dendron conjugates produce less singlet oxygen per quanta of absorbed light, their increased absorption of light in comparison to single porphyrins is sufficient to overcome this in a therapeutic context. For this reason, the singlet oxygen generation potential of each structure was calculated by multiplying the absorption ratio by  $\Phi_{\Delta}$  in order to accurately reflect the hypothetical total production of singlet oxygen of the entire porphyrin-dendron structure in an abundance of light, such as in clinical use. Comparison of these values demonstrates that the overall therapeutic efficacy of the structures increases with increasing porphyrin loading. Despite this increase, only **9** has a singlet oxygen generation potential in excess of its parent porphyrin **11**.

For this reason, **9** was selected as the most promising candidate for development into a high-potency therapeutic. It was envisaged that replacing the triethylene glycol spacer with a PEG<sub>6</sub> chain would increase hydrophilicity and facilitate bioconjugation. Thus, synthesis of an analogue of **3** with a longer PEG chain was carried out. Synthesis of **12** (Fig. 6) was carried out via the same peptide coupling methodology as **3** to afford **12** in moderate yield.

**Figure 6.** Synthetic scheme for structures **12-14**. i, **5**, CuSO<sub>4</sub>, NaAsc, TBTA, 40°C, MW, ii, TFA, 40°C. iii, imidazole-1-sulfonyl azide hydrogen sulfate, copper (II) sulfate pentahydrate, 40°C.

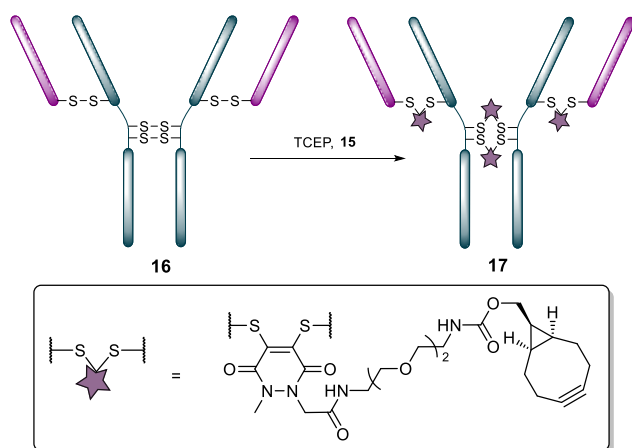


Similarly, the synthesis of **13** was carried out under identical conditions to **9**, with microwave irradiation at 40°C yielding the desired product without chromatographic purification, followed by immediate deprotection of the Boc protecting group. Finally, to allow for bioconjugation under previously optimised conditions, azide functionalisation of the amine focal point was carried out.<sup>7</sup> **14** was prepared utilising a diazotransfer reagent (imidazole-1-sulfonyl azide) previously shown to be compatible with porphyrins.<sup>20</sup> The reaction was monitored by HPLC, and **14** was obtained in good yield after workup.

With **14** in hand, bioconjugation to the HER2-targeting antibody trastuzumab<sup>®</sup> was explored. As well as demonstrating clinical relevance as both a therapeutic antibody and in the clinical ADC Kadcyla<sup>®</sup>,

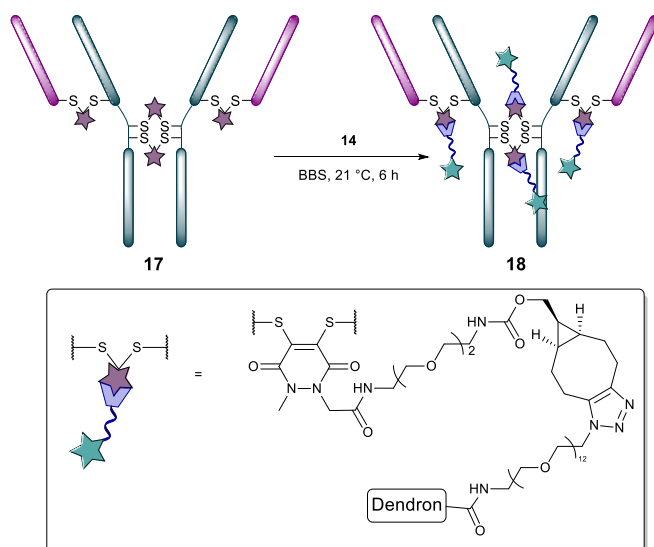
trastuzumab<sup>®</sup> also acts as an excellent model for bioconjugation to other IgG1 antibodies, demonstrating the versatility of this bioconjugation method for new and existing disease targets. Initially, functional re-bridging on the four solvent-accessible disulfide bridges was performed through concomitant reduction with TCEP and the strained alkyne functionalised pyridazinedione **15** (Fig. 7) for 16 hrs at 4 °C. UV analysis confirmed a DAR of *ca* 4.

**Figure 7.** Schematic representation of the functional rebridging of trastuzumab with pyridazinedione **15**.



Subsequent strain-promoted (SPAAC) attachment of **14** was carried out at 21°C for 6 hours, followed by gel filtration to remove excess reagents (Fig. 8). UV analysis was performed on conjugate **18**, to determine an average DAR of 15.4 porphyrins per antibody, close to the theoretical maximum of 16 across the 4 interchain disulfide bridges. Further analysis by SDS-PAGE demonstrates complete re-bridging of the bioconjugate, with no partial re-bridging or unconjugated antibody fragments at lower molecular weight observed.

**Figure 8.** Schematic representation of strain-promoted click conjugation of the azide-functionalised dendron **14** onto functionalised bioconjugate **17**.

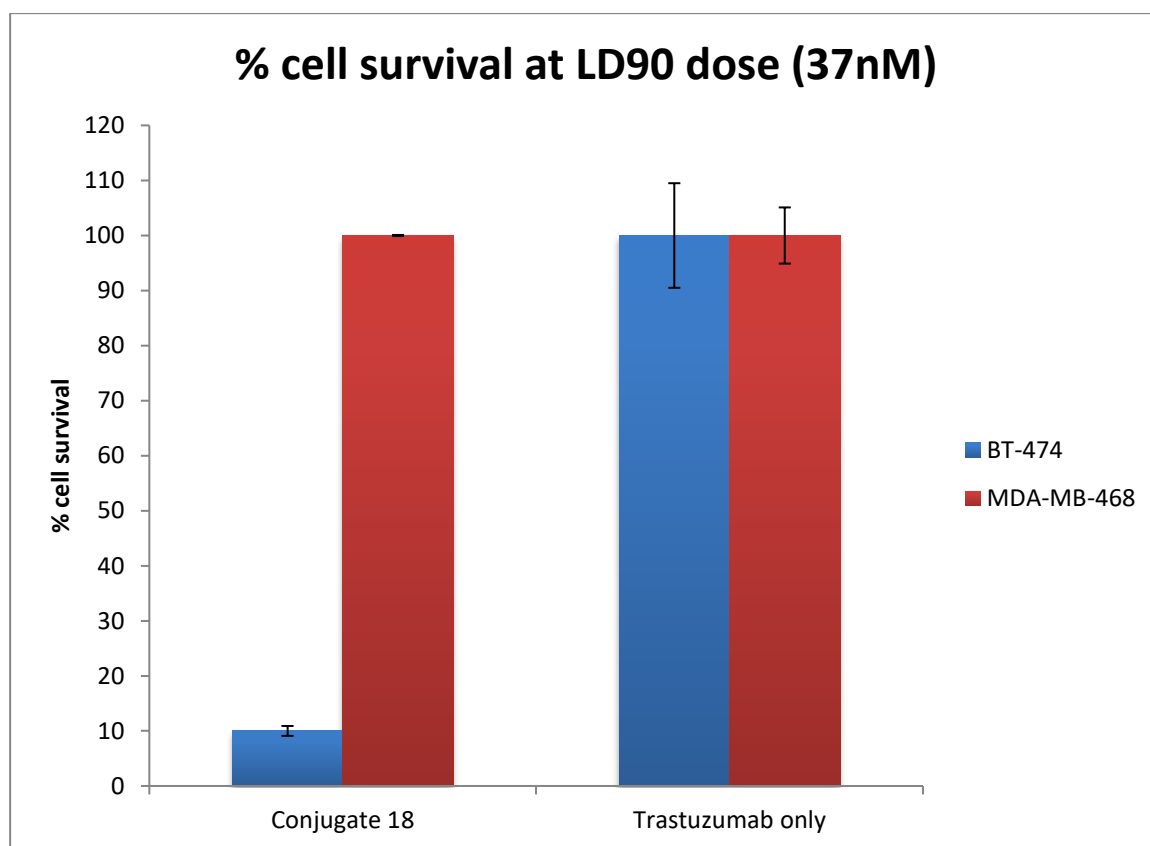




Following successful bioconjugation, we next appraised the efficacy of the synthesised ADC *in vitro* on cell lines which overexpress (BT-474) and express native levels of HER2 receptor (MDA-MB-468), using unmodified trastuzumab<sup>®</sup> as a control. (Fig. 9) As in our previous work,<sup>7</sup> *in vitro* experiments were carried out utilising broad spectrum illumination (20 J cm<sup>-2</sup>) rather than red / near IR light. This allows a more accurate reflection of the potency of the conjugate in a clinical setting, where the use of biomedical lasers compensates for the reduced absorption of the porphyrins in the red region through light fluences which are orders of magnitude greater.

Under these conditions, conjugate **18** demonstrated an impressive photocytotoxic effect against the HER2 overexpressing cells, with a nanomolar LD<sub>90</sub> value, while at the same concentration leaving HER2- cells unaffected (Fig. 9). In both cases, the control native trastuzumab displayed no cytotoxicity at these concentrations. In addition, **18** displayed no dark toxicity in both cell lines even at the highest concentration used (1 μM) (see ESI).

**Figure 9.** Graph demonstrating cell survival of BT-474 and MDA-MB-468 cell lines following incubation with either conjugate **18** or unmodified trastuzumab<sup>®</sup> control at the LD<sub>90</sub> dose, and irradiation (20 J cm<sup>-2</sup>) (Full cytotoxicity data is available in ESI).



In conclusion, we have demonstrated the first synthesis of a range of click-enabled porphyrin-dendron multipliers for bioconjugation applications, with a mild and facile synthetic procedure. Following evaluation of the photophysical characteristics of these structures, we selected a lead candidate and optimised bioconjugation using the HER2-targeting clinical antibody trastuzumab<sup>®</sup>. Subsequent *in vitro* biological evaluation confirmed the selectivity and potency of this porphyrin photoimmunoconjugate, with a remarkable nanomolar LD<sub>90</sub> value on HER2 overexpressing cells, and no observable effect on cells that express native HER2 levels, nor dark cytotoxicity, at the same concentration. The clear lack of effect from the trastuzumab<sup>®</sup> control at the LD<sub>90</sub> value, and in the

absence of light, shows cytotoxic action is promoted only by light activation of the photosensitisers. The large differential seen between HER2 overexpressing cells, and those with native HER2 levels (Fig. 9) confirms receptor binding is unaffected by conjugation of the porphyrin dendron. Clearly, trastuzumab<sup>®</sup> is well known to elicit an anticancer effect on HER2 positive tumours, and is routinely used in the clinic. The results presented here offer an exciting potential for augmenting the therapeutic effects of trastuzumab<sup>®</sup> by controlled conjugation of photosensitiser dendrons to this antibody.

## Materials and methods

**General peptide coupling method:** To a stirred solution of dendron acid (1.1 mmol) in dichloromethane (100 mL) was added tert-butyl (2-(2-(2-aminoethoxy)ethoxy)ethyl)carbamate (0.272 g, 1.1 mmol) in dichloromethane (50 mL). DIPEA (0.35 mL, 2.5 mmol) was added, followed by addition of PyBOP (0.572 g, 1.1 mmol), and the mixture was stirred at rt overnight. The solvent was removed under reduced pressure and the crude material purified by column chromatography (silica, 5% MeOH:DCM) to yield the product as a colourless oil.

**General microwave click method:** To a 10 mL microwave tube was added zinc 5-[4-azidophenyl]-10,15,20-tri-(N-methyl-4-pyridinium)porphyrin trichloride (2-4 equivalents) and dendron **1-3** (19 mg, 0.022 mmol) in tBuOH:water (1:1, 8 mL). Copper (II) sulfate pentahydrate (5 mg), sodium ascorbate (5 mg), and TBTA (1 mg) was added, and the mixture heated to 40°C by MW (75W, max pressure 100 bar, max stirring) for 1 hour. The mixture was concentrated under reduced pressure, and ammonium hexafluorophosphate added to the mixture. The resulting solution was filtered and the precipitate re-dissolved in acetone. Tetrabutylammonium chloride was added, and the resulting solution filtered. The product was precipitated from diethyl ether over MeOH to yield the product as a green solid.

## Supporting Information

The Supporting Information is available free of charge on the ACS Publications website at DOI:

Synthesis and analytical data for compounds 1-14, bioconjugation and analytical data for conjugates 16-18, photophysical and cytotoxicity data.

The authors declare no competing financial interest.

## References

- (1) Mullard, A. (2013) Maturing antibody-drug conjugate pipeline hits 30. *Nat. Rev. Drug Discov.* **12**, 329-332.
- (2) Beck, A., Goetsch, L., Dumontet, C., Corvaia, N. (2017) Strategies and challenges for the next generation of antibody-drug conjugates. *Nat. Rev. Drug Discov.* **16**, 315-337.
- (3) Josefsen, L. B., Boyle, R. W. (2008) Photodynamic therapy and the development of metal-based photosensitisers. *Met. Based Drugs* **2008**, 276109.

- (4) Baldwin, A. D., Kiick, K. L. (2011) Tunable Degradation of Maleimide–Thiol Adducts in Reducing Environments. *Bioconj. Chem.* **22**, 1946-1953.
- (5) Shen, B.-Q., Xu, K., Liu, L., Raab, H., Bhakta, S., Kenrick, M., Parsons-Reponte, K. L., Tien, J., Yu, S.-F., Mai, E., et al. (2012) Conjugation site modulates the in vivo stability and therapeutic activity of antibody-drug conjugates. *Nat. Biotechnol.* **30**, 184.
- (6) Alley, S. C., Benjamin, D. R., Jeffrey, S. C., Okeley, N. M., Meyer, D. L., Sanderson, R. J., Senter, P. D. (2008) Contribution of Linker Stability to the Activities of Anticancer Immunoconjugates. *Bioconj. Chem.* **19**, 759-765.
- (7) Tumeý, L. N., Charati, M., He, T., Sousa, E., Ma, D., Han, X., Clark, T., Casavant, J., Loganzo, F., Barletta, F., et al. (2014) Mild Method for Succinimide Hydrolysis on ADCs: Impact on ADC Potency, Stability, Exposure, and Efficacy. *Bioconj. Chem.* **25**, 1871-1880.
- (8) Smith, M. E. B., Caspersen, M. B., Robinson, E., Morais, M., Maruani, A., Nunes, J. P. M., Nicholls, K., Saxton, M. J., Caddick, S., Baker, J. R., et al. (2015) A platform for efficient, thiol-stable conjugation to albumin's native single accessible cysteine. *Org. Biomol. Chem.* **13**, 7946-7949.
- (9) Maruani, A., Smith, M. E. B., Miranda, E., Chester, K. A., Chudasama, V., Caddick, S. (2015) A plug-and-play approach to antibody-based therapeutics via a chemoselective dual click strategy. *Nat. Commun.* **6**, 6645.
- (10) Robinson, E., Nunes, J. P. M., Vassileva, V., Maruani, A., Nogueira, J. C. F., Smith, M. E. B., Pedley, R. B., Caddick, S., Baker, J. R., Chudasama, V. (2017) Pyridazinediones deliver potent, stable, targeted and efficacious antibody-drug conjugates (ADCs) with a controlled loading of 4 drugs per antibody. *RSC Adv.* **7**, 9073-9077.
- (11) Maruani, A., Savoie, H., Bryden, F., Caddick, S., Boyle, R., Chudasama, V. (2015) Site-selective multi-porphyrin attachment enables the formation of a next-generation antibody-based photodynamic therapeutic. *Chem. Commun.* **51**, 15304-15307.
- (12) Bryden, F., Maruani, A., Savoie, H., Chudasama, V., Smith, M. E. B., Caddick, S., Boyle, R. W. (2014) Regioselective and Stoichiometrically Controlled Conjugation of Photodynamic Sensitizers to a HER2 Targeting Antibody Fragment. *Bioconj. Chem.* **25**, 611-617.
- (13) Swavey, S., Tran, M. (2013) Porphyrin and Phthalocyanine Photosensitizers as PDT Agents: A New Modality for the Treatment of Melanoma, in *Recent Advances in the Biology, Therapy and Management of Melanoma* (Davids, L. M., Ed.) pp Ch. 11, InTech, Rijeka.
- (14) Anami, Y., Xiong, W., Gui, X., Deng, M., Zhang, C. C., Zhang, N., An, Z., Tsuchikama, K. (2017) Enzymatic conjugation using branched linkers for constructing homogeneous antibody-drug conjugates with high potency. *Org. Biomol. Chem.* **15**, 5635-5642.
- (15) Chow, S. Y. S., Lo, P.-C., Ng, D. K. P. (2016) An acid-cleavable phthalocyanine tetramer as an activatable photosensitizer for photodynamic therapy. *Dalton Trans.* **45**, 13021-13024.
- (16) Chow, S. Y. S., Zhao, S., Lo, P.-C., Ng, D. K. P. (2017) A cell-selective glutathione-responsive tris(phthalocyanine) as a smart photosensitizer for targeted photodynamic therapy. *Dalton Trans.* **46**, 11223-11229.
- (17) Morosini, V., Frochot, C., Barberi-Heyob, M., Schneider, R. (2006) Divergent synthesis of novel unsymmetrical dendrons containing photosensitizing units. *Tetrahedron Lett.* **47**, 8745-8749.
- (18) Giuntini, F., Bryden, F., Daly, R., Scanlan, E. M., Boyle, R. W. (2014) Huisgen-based conjugation of water-soluble porphyrins to deprotected sugars: towards mild strategies for the labelling of glycans. *Org. Biomol. Chem.* **12**, 1203-1206.
- (19) Dash, B. P., Satapathy, R., Bode, B. P., Reidl, C. T., Sawicki, J. W., Mason, A. J., Maguire, J. A., Hosmane, N. S. (2012) "Click" Chemistry-Mediated Phenylene-Cored Carborane Dendrimers. *Organometallics* **31**, 2931-2935.
- (20) Bryden, F., Boyle, R. W. (2013) A Mild, Facile, One-Pot Synthesis of Zinc Azido Porphyrins as Substrates for Use in Click Chemistry. *Synlett* **24**, 1978-1982.

## TOC image

